Requirements for a Transportation System Based on Ultrasonic Traveling Waves Using the Measurement of Spatial Phase Difference

Jie Zhao[1], Guanyu Mu[1], Huijuan Dong[1]*, Tong Sun[2] and Kenneth.T.V. Grattan[2]*

1. State Key Laboratory of Robotics and System, Harbin Institute of Technology, Harbin, 150001, Heilongjiang Province, China

2. School of Mathematics, Computer Science and Engineering, City, University of London, London, EC1V 0HB, UK

Corresponding Author.

E-mail address: dhj@hit.edu.cn (H. Dong) K.T.V.Grattan@city.ac.uk (K.T.V. Grattan)

Abstract: Having good control over the speed and direction of non-contact transportation is critical in industry today, especially in areas such as the manufacturing of flat display panels, silicon wafers of semi-silicon and a number of other electronic devices. In a dual transducer-type ultrasonic levitation-based transportation system, it is well known that the vibrating plate length and the wavelength of the flexural vibration should satisfy a strict relationship, i.e. one given by the spatial phase difference, ϕ, so that the transportation process could be as fast as possible and therefore most effective for industry. However, it is difficult to obtain the value of ϕ through calculation, or through making adjustments during the operation of the transportation process. In this paper, the relationship across the temporal phase shift, θ, the spatial phase difference, ϕ, and the Standing Wave Ratio (SWR), which directly controls the speed and direction of the transportation system, was derived by the authors for the first time. Subsequently, experimental solutions for the measurement of ϕ were obtained in this work, using a Laser Doppler Vibrometer-based approach (LDV) and as a result, the research has been successful in giving results for ϕ, through the series of experiments carried out and reported.

Keywords: dual transducer-type levitation-based transportation system, LDV-based measurements, measurement of the spatial phase difference, temporal phase shift

1. Introduction

Non-contact transportation systems based on ultrasonic levitation have many potential applications in industry, such as in manufacturing display panels, silicon wafers of semi-silicon and a number of other electronic devices[1, 2]. Unlike air pressure systems or magnetic-based systems, ultrasonic transportation systems show a number of important characteristics, such as having a simple configuration and use over long transportation distances being possible, with no limitations on the materials used, as well as allowing docking at arbitrary points. Compared to early SW (Standing Wave)-induced ultrasonic transportation systems[3-14], the dual transducer-type ultrasonic levitation-based transportation system is capable of generating a mixture of both SWs and TWs (Traveling Waves). This means that the transportation direction and the velocity of this system can be easily controlled by adjusting the direction and component of the TWs (defined as the Standing Wave Ratio, SWR).

It has been reported that both pure TWs and a mixture of TWs and SWs can be propagated on the vibrating plate, using two excitation modes. In these early studies[15, 16], one of these two modes, the Exciter-Absorber mode, has been developed to create pure TWs. In a typical setup used to generate this mode, one transducer was mounted and used as the exciter at one end of the vibrating plate, and two bars of silicone rubber were securely attached to the other end, to absorb the vibration generated by the transducer. However, it was found to be difficult to adjust the speed and direction of the waves being propagated when the system was in operation, because this kind of absorbing material could not easily be changed. An alternative setup of the Exciter-Absorber mode is possible, in which the absorbing material has been replaced by a transducer, used in an absorber role. In this way, its capacity for absorbing vibration could easily be adjusted through the parameters of the circuit connected to the transducer[17]. By comparison to the setup in which the absorbing material was used, its speed could be readily adjusted, but it was still difficult to reverse the direction of the waves, in operation, because switching the roles of both transducers was difficult. Alternatively, the second of these two excitation modes, the Exciter-Exciter mode[18-21] has also been implemented and so the pure TWs could be generated by adjusting the temporal phase shift, θ, of the voltage being applied to both the transducers, at the same frequency. As a result, this method has allowed the control of the direction of the pure TWs on the vibrating plate[22-24].

In these studies, the principles of the generation of pure TWs are discussed [23, 25]. However, adjusting the TW component (SWR) of the vibration is equally important when controlling the speed of the transportation. Thus, it is essential to establish the correct theoretical relationship between the values of the SWR and the temporal phase shift, θ. Thus in this research program, it has been shown by the authors that the SWR is not only related to θ, but also to the spatial phase difference, ϕ (defined by the relationship between the vibrating plate length, L, and the wavelength, λ) as well. However, ϕ is difficult to obtain, either by direct measurement or through calculation. By comparison, the temporal phase shift, θ, can easily be programmed during the actual transportation process. Therefore, the authors show that the SWR can be adjusted by using θ and to do so, ϕ should be obtained prior to the transportation experiments being carried out. Specifically, the relationship across θ, ϕ and the SWR has first been derived by the authors, after which a novel way of measuring the spatial phase difference, ϕ, is provided. Finally, a series of experiments has been carried out by the authors to demonstrate the requirements for the TWs being propagated, these being important for the control of such a transportation system for industry.

2. Relationship of θ and ϕ To The SWR

It is well known that a dual-transducer system can be excited in two different modes to generate waves, one of which is an Exciter-Exciter mode that can be implemented by applying a voltage, with a certain phase shift, but at the same frequency to both the transducers. Consequently, the travelling waves (TWs) and the standing waves (SWs) can occur simultaneously along the whole plate, when an appropriate value of the SWR is set, where this is defined as the ratio between the energy of the Standing Waves and that of the Travelling Waves. Thus, the SWR is a key parameter for the use of the transportation system, as it is a function of both the transportation speed and the levitation force. It is important to note that the SWR is related not only to the temporal phase shift, θ, between the two transducers but also to the spatial phase difference, ϕ. The theoretical relationship across these three parameters is now derived, as

shown below.

2.1 Analytical study of the waves on the vibrating plate

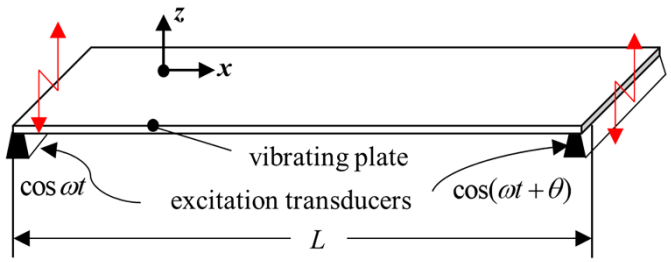

Fig. 1 Schematic of the Exciter-Exciter mode of the ultrasonic transportation device

Fig. 1 illustrates the key principles of the ultrasonic transportation device, when operating in the Exciter-Exciter mode. When the vibrations of the two transducers are overlapped and the contribution of the evanescent waves is neglected, the z direction-based vibration velocity of the plate at a time, *t*, and at a position, *x*, can be written as[23]:

$$\begin{aligned} v(x,t) &= A_0(\cos\omega t\cos kx + \cos(\omega t+\theta)\cos[k(L-x)]) \\ &= A_0(\cos\omega t\cos kx + \cos(\omega t+\theta)\cos(kx-\phi)) \end{aligned} \tag{1}$$

where k and ω respectively represent the wavenumber of the vibration velocity and the angular frequency applied to both the transducers and A_0 is the wave amplitude. L is the length of the vibrating plate and ϕ is termed the spatial phase difference, given by $k(L\text{-}n\lambda)$, where λ is the wavelength of this vibrating plate and n is an integer. During the process of transportation, these two transducers illustrated in Fig. 1 are excited at a frequency, ω, with a phase shift, θ, at an amplitude of A_0, to generate the wave being propagated along the vibration plate, of length L.

The standing wave ratio (SWR) is defined in the literature[25] as:

$$SWR = \frac{v_{\max}}{v_{\min}} \tag{2}$$

where $v_{\max}$ and $v_{\min}$ are respectively the maximum and minimum values of the amplitude of $v(x,t)$, which can be derived from (1). Accordingly, the analytical expression for the SWR, given as a function of θ and ϕ, has also been developed by the authors in this work, noting that previous studies have rarely focused on this important relationship.

2.2 Location of x_0 on the vibrating plate where the maximum/minimum amplitudes occur

The location, x_0, at a time, t, where $v_{\max}$ or $v_{\min}$ occurs, can be obtained by setting the partial derivatives of $v(x,t)$ for x to be zero, as shown in (3):

$$\frac{\partial v(x,t)}{\partial x} = 0 \tag{3}$$

$$\tan x_0 = \frac{\sin\phi\cos(\omega t+\theta)}{\cos\omega t+\cos(\omega t+\theta)\cos\phi} \tag{4}$$

Equation (4) implies that the location, x_0, is related not only to θ and ϕ, but also to the time, t. In order to calculate the value of the SWR, it is essential to obtain the value of the amplitude of $v_{\max}$ or $v_{\min}$, at position x_0, seen in (4), as discussed specifically below.

2.3 Value of the amplitude of the vibration velocity at position, x_0

Substituting the value of x_0, obtained by using (4), into $v(x,t)$ (from (1)), the vibration velocity at this position, $v_{x0}(t)$, can be expressed as shown below:

$$v_{x_0}(t)=A_0\sqrt{\cos^2\omega t+\cos^2(\omega t+\theta)+2\cos\omega t\cos(\omega t+\theta)\cos\phi} \tag{5}$$

The amplitude of $v_{x0}(t)$ can subsequently be calculated through the time derivative, t, shown as (6). Following (6), the time at which this occurs, t_0, can be determined using (7) when $v_{x0}(t)$ approaches a maximum or minimum:

$$\frac{\mathrm{d}}{\mathrm{d}t}v_{x_0}(t)=0 \tag{6}$$

$$(\cos\phi+\cos\theta)\sin(2\omega t_0+\theta)=0 \tag{7}$$

Finally, substituting the value of time, t_0, from (7) into (5), the normalized maximum and minimum velocity values, $\hat{v}_{xmax}$ and $\hat{v}_{xmin}$, can be given by:

$$\begin{aligned}\hat{v}_{x\max}&=\max\left(\left|2\sin\frac{\phi}{2}\sin\frac{\theta}{2}\right|,\left|2\cos\frac{\phi}{2}\cos\frac{\theta}{2}\right|\right)\\ \hat{v}_{x\min}&=\min\left(\left|2\sin\frac{\phi}{2}\sin\frac{\theta}{2}\right|,\left|2\cos\frac{\phi}{2}\cos\frac{\theta}{2}\right|\right)\end{aligned} \tag{8}$$

2.4 Value of the Standing Wave Ratio (SWR)

Equation (8) clarifies the influence of θ and ϕ on the values of $\hat{v}_{xmax}$ and $\hat{v}_{x\min}$. Considering the range of values of θ in (8), the SWR can be written as:

$$SWR=\begin{cases}\left|\cot\frac{\phi}{2}\cot\frac{\theta}{2}\right| & 0<\theta<\pi-\phi,\quad \pi+\phi<\theta<2\pi\\ \left|\tan\frac{\phi}{2}\tan\frac{\theta}{2}\right| & \pi-\phi<\theta<\pi+\phi\end{cases} \tag{9}$$

Both (8) and (9) demonstrate clearly that θ and ϕ determine the value of the SWR. Both the velocity and the direction of the transportation system then can be controlled using θ, when ϕ is determined. Thus, to do so, it is critically important to obtain the value of ϕ in this case.

3. Method to measure ϕ using a Laser Doppler Vibrometer (LDV)

As mentioned above, the spatial phase difference, ϕ, is difficult to obtain, either by calculation or direct measurement. Based on a knowledge of (8) and (9), a novel indirect method for measuring ϕ is described by the authors in this work. Specifically, a set of the maximum and minimum values of the amplitudes of the vibration velocity over the vibrating body, i.e. $\hat{v}_{x\max}$ and $\hat{v}_{x\min}$, can be also obtained through the use of a scanning Laser Doppler Vibrometer (type Polytech PSV-500B), when the temporal phase shift, θ, of the voltage being applied to the two transducers varies from 0 to 2π, over known intervals of 10 degrees. Subsequently, ϕ can be calculated by using only these obtained amplitudes, as seen from (8).

Accordingly, the values of $\hat{v}_{xmax}$, $\hat{v}_{xmin}$ as a function of θ, under the conditions of different values of ϕ, are plotted in Fig. 2. (where ϕ is given in graphs (a), (b), (c) and (d) respectively).

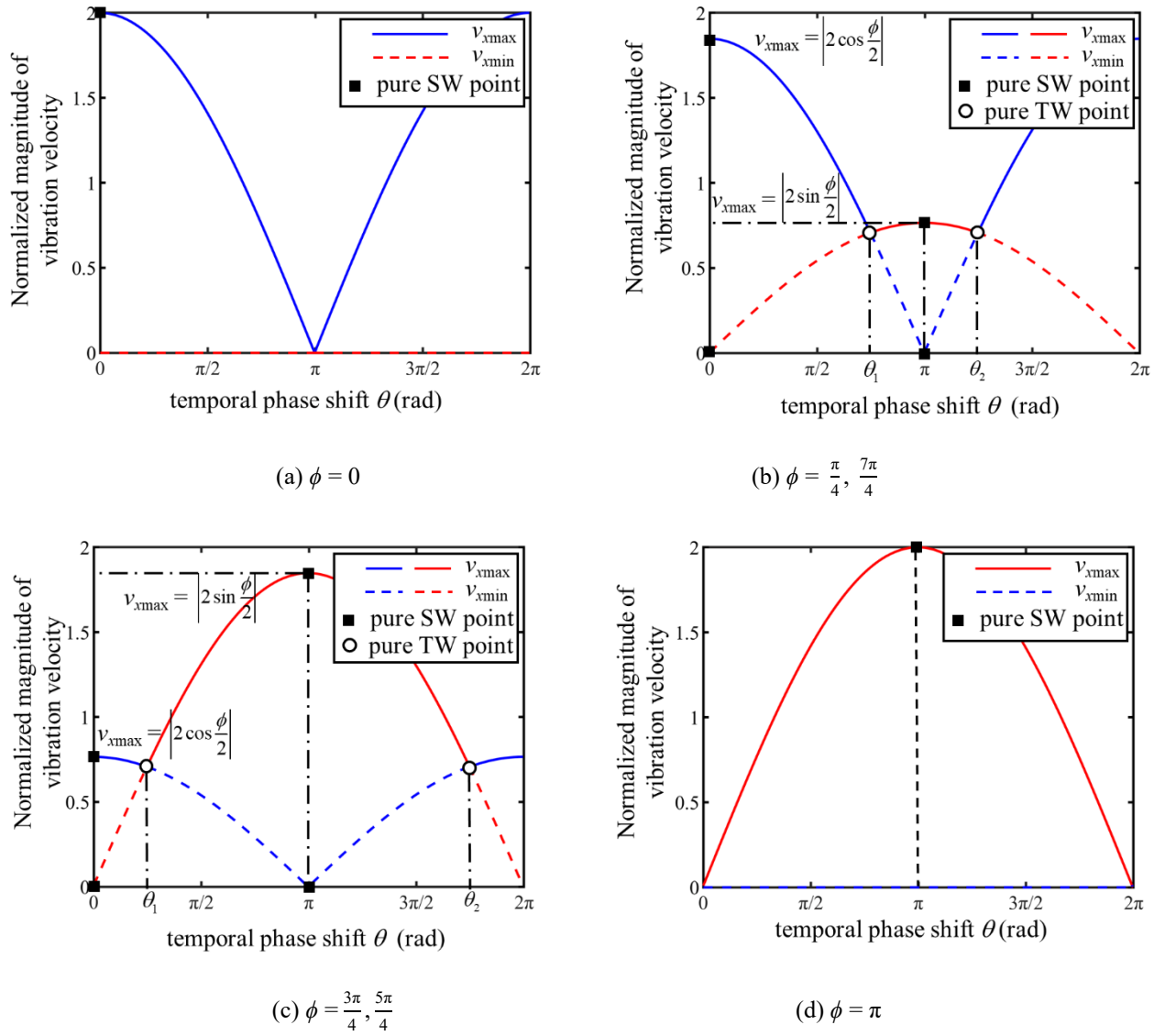

(a) $\phi = 0$ (b) $\phi = \frac{\pi}{4}, \frac{7\pi}{4}$

(c) $\phi = \frac{3\pi}{4}, \frac{5\pi}{4}$ (d) $\phi = \pi$

Fig. 2. Theoretical relationships between $\hat{v}_{xmax}$ (solid line), $\hat{v}_{xmin}$ (dotted line) against θ under the conditions where the spatial phase values are (a) $\phi = 0$, (b) $\phi = \frac{\pi}{4}, \frac{7\pi}{4}$, (c) $\phi = \frac{3}{4}\pi, \frac{5\pi}{4}$ and (d) $\phi = \pi$.

3.1 SW-based approach to measurement of ϕ

As can be seen from Fig. 2 and (8), by cross-comparing $f(\theta) = \left|2\cos\frac{\phi}{2}\cos\frac{\theta}{2}\right|$ (shown in blue on the graph) with $g(\theta) = \left|2\sin\frac{\phi}{2}\sin\frac{\theta}{2}\right|$ (this being in red) at a given value of θ, the larger value denotes $\hat{v}_{max}$ (solid line on the graphs) and similarly, the smaller value is $\hat{v}_{min}$ (dotted line on the graphs). Clearly, *f(θ)* and *g(θ)* approach the amplitudes of $\left|2\cos\frac{\phi}{2}\right|$ and $\left|2\sin\frac{\phi}{2}\right|$ when θ has values of 0 and π respectively. It can be noted that the SW is formed along the vibrating plate, marked using solid squares in the graphs (a) to (d) in Fig. 2. In practice, these amplitudes can also be measured by using the Laser Doppler Vibrometer (LDV). As a result, ϕ can be calculated from a knowledge of both $\left|2\cos\frac{\phi}{2}\right|$ and $\left|2\sin\frac{\phi}{2}\right|$, which were obtained by normalizing the measured amplitudes of the SWs, this method being

termed by the authors 'the SW-based method'.

In summary therefore, this method of measuring ϕ is simple because the values of $\hat{v}_{max}$ are measured only twice under the two SW-induced conditions where the phase shift, θ, is given by 0 and π. However, as Fig.2 (b) shows, the distribution of the vibration is identical for the two symmetric values of ϕ with respect to π, which are equal to $\frac{\pi}{4}$, $\frac{7\pi}{4}$, and thus it is difficult to tell which one is real by using this method. The same situation is seen in Fig.2 (c). In order to resolve this problem, a TW-based approach which offers a solution to the measurement of ϕ is given, where the range of ϕ can be derived from the direction of the TWs generated, as discussed below.

3.2 TW-based approach to measurement of ϕ

The TW-based measurement method has been inspired by the following principle. As can be seen from Fig. 2, each position on the vibrating plate shares the same amplitude of the vibration velocity ($\hat{v}_{max}=\hat{v}_{min}$) at the intersection points of *f(θ)* and *g(θ)* (which are marked with hollow circles in Graphs (b) and (c), in Fig. 2). This indicates that the pure TWs on the vibrating plate are generated at a unique pair of values of the phase shifts, θ_1 and θ_2, for each value of ϕ. Specifically, the values of θ, i.e., θ_1 and θ_2 seen in Fig. 2(b), can be acquired when generating a pure TW, which can be detected by using the LDV method discussed earlier. This means that ϕ can be also given by (10), which describes the relationship between ϕ and the TW-based phase shifts, θ_1 and θ_2, derived from (8):

$$\phi=\begin{cases}\pi-\theta_1=\theta_2-\pi & 0<\phi<\pi\\ \pi+\theta_1=3\pi-\theta_2 & \pi<\phi<2\pi\end{cases} \tag{10}$$

Therefore, according to (10), the spatial difference, ϕ, can be obtained by measuring the TW-based phase shifts, θ_1 or θ_2. However, whether the value of ϕ is smaller or greater than π still needs to be determined.

When the temporal phase shift is given by θ_1 or θ_2, the two pure TWs are induced in opposite directions along the vibrating plate, with their vibration velocity being expressed as:

$$\hat{v}(x,t)=\sin\phi\sin(\pm\omega t-kx+\phi) \tag{11}$$

As can be seen from (11), the propagation direction of the TWs can be used to determine the range of values of ϕ (which are either smaller or greater than π). As shown in Fig. 3, the red zone represents the positive direction, while the green zone stands for the negative direction. Specifically, when $0\leq\phi<\pi$, the pure TWs at θ_1 and θ_2 represent the positive and negative directions respectively, as shown in Fig. 3(a), and verse versa for $\pi\leq\phi<2\pi$, as shown in Fig. 3(b). Therefore, the actual value of ϕ can be determined by combining (10) and the directions of the TWs.

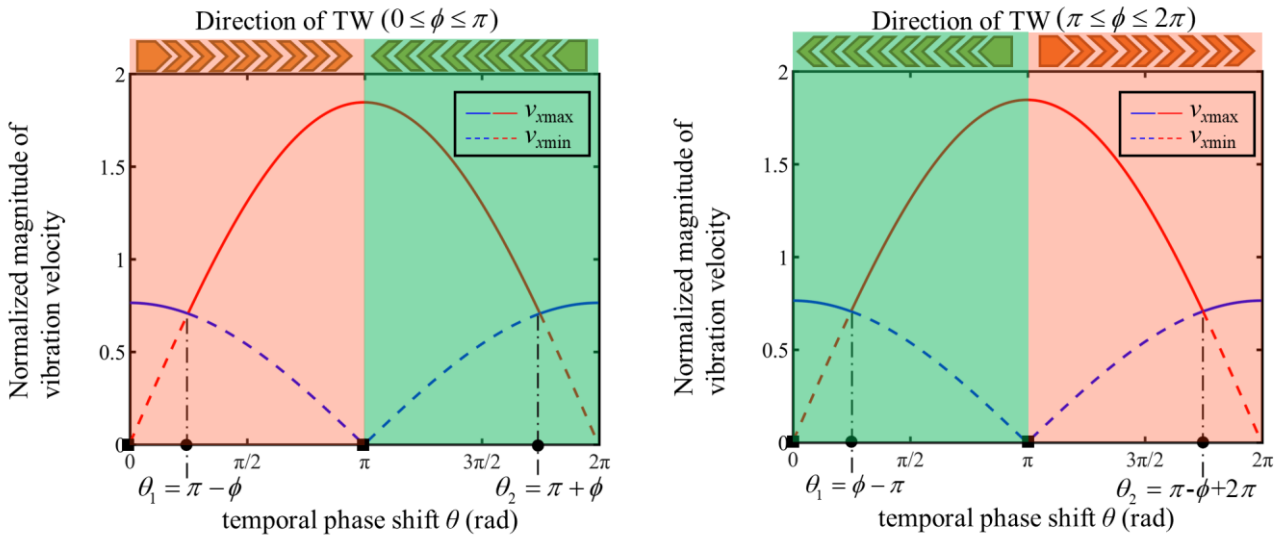

(a) $\phi = \frac{3\pi}{4}$ $(0 \le \phi < \pi)$ (b) $\phi = \frac{5\pi}{4}$ $(\pi \le \phi < 2\pi)$

Fig. 3. Relationship (a) and (b) between θ and the directions of the TWs ($\phi = \frac{\pi}{4}, \frac{7\pi}{4}$, where the red and green zones represent the positive and negative directions respectively).

In summary, both the SW-based and TW-based methods for measuring ϕ are detailed in this work, through the relationship between ϕ, θ, and the SWR. The SW-based method is valid when ϕ is equal to 0 or π, and therefore only suitable when the length of the vibrating plate is equal to an integer multiple of the wavelength (L=n$\frac{\lambda}{2}$, n=1, 2, ...); while the TW-based method is suitable for the rest length of the vibrating plate ($L \neq$n$\frac{\lambda}{2}$, n=1, 2, ...). Subsequently, a series of experiments has been carried out to demonstrate the measurement of ϕ, as discussed in Section IV below.

4. System Configuration

Fig. 4 (a) and (b) show photographs of the dual transducer-type ultrasonic levitation-based transportation system considered in this work, which is composed of a vibrating plate and two Langevin-type transducers. In the experiments carried out, the two transducers were driven using a power supply developed by the authors[26] (dual channels, 200W, 0-120V, 0-100kHz, 0-360°), at a frequency of 32.846kHz. Here the vibrating plate used in this work was of 3mm thickness, 35mm width and length, L, of 300mm, and was mounted on the transducers. Then the amplitudes of the vibration velocities along the vibrating plate, were measured by the using the scanning LDV (type PSV-500-B, Polytec) system. As a result, values of ϕ can be obtained from a knowledge of $\hat{v}_{max}$ or the temporal shifts.

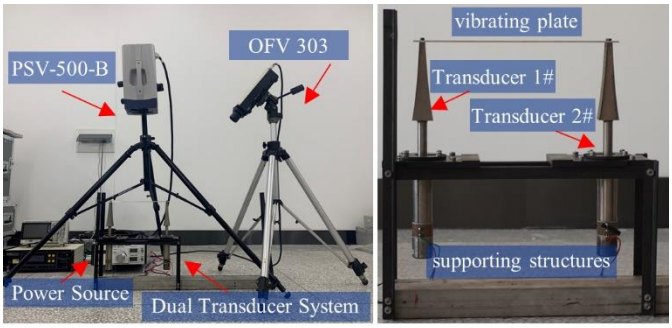

Fig. 4. Photograph of the dual transducer-type transportation device (where h=3mm, w=35mm, L=300mm) showing (a) the two

transducers #1 and #2, the vibrating plate and the supporting structures and (b) the use of the LDV system described.

5. Experimental verification

5.1 Measurement of ϕ using the SW-based method

In order to obtain the values of ϕ, $\hat{v}_{max}$ can be measured with the temporal phase shifts, θ, being set to 0 and π. Here, the working frequency of the transducers was locked to 32.846kHz[26], which is shifted a little from the designed frequency. In order to visualize the SWs and TWs along the vibrating plate, a single point LDV (type OFV-303, Polytec) was connected to the scanning LDV simultaneously as a reference signal input, to obtain the phase information on the vibration velocities. As a result, Fig. 5 shows the distributions of the z-direction vibration velocities on the middle part of the vibrating plate, corresponding to the range of 88mm-205mm, measured by using the scanning LDV. Following that, the values of SWR were 27.71, 2.93, 70.08, 4.03 (when θ equals 0° , 50°, 180°, 310°), these being calculated using the data from the LDV. As can be seen from Fig. 5 (a), (c), the SWs, whose wavelength, λ, were ~28mm were formed when θ equals 0 and 180°, while in Fig. 5 (b), (d), the two TWs of opposite direction are formed on the vibrating plate at θ equals 50° and 310° respectively. It is important to note that the values of 50° and 310° are symmetric about π (180°).

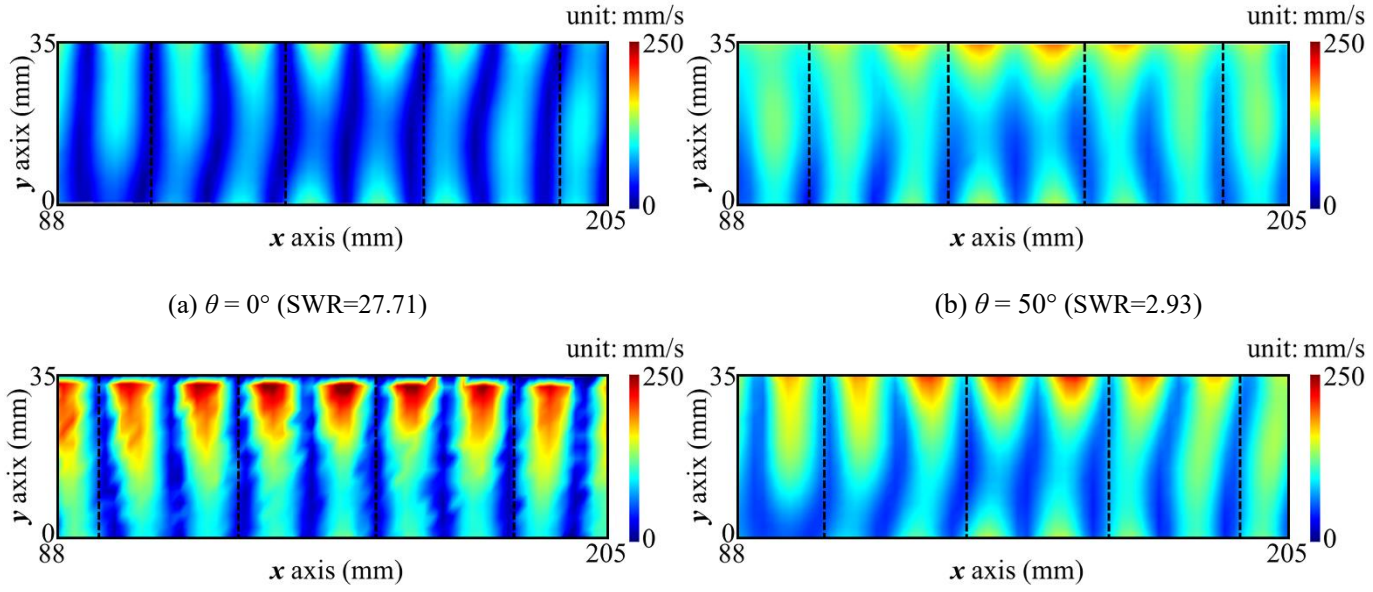

(a) θ = 0° (SWR=27.71)

(b) θ = 50° (SWR=2.93)

(c) θ = 180° (SWR= 70.08)

(d) θ = 310° (SWR= 4.03)

Fig. 5. The velocity distribution along the vibrating plate measured by using the scanning LDV shown in Fig.4. (f=32.846kHz, L=300mm, Vpp=30V, where θ = 0°, 50°, 180°, 310° in graphs (a) to (d) respectively)

Then by providing the reference signal input from the single point LDV in this case, the averaged amplitudes and phases of the vibration velocities could be extracted from Fig. 5, as plotted in Fig. 6, where the solid lines represent the theoretical values, and the hollow circles and squares shown represent the experimental values. As can be seen in Fig. 6(a), the phase shift periodically steps between -π and π, which implies that the SWs have been formed at a value of θ equal to 0°[27]. The amplitude, $\left|2\cos\frac{\phi}{2}\right|$, of the SW was 0.00258mm/s (average value along the y-direction). Similarly, at θ equals 180°, the amplitude of the SW, $\left|2\sin\frac{\phi}{2}\right|$, changes to 0.00541mm/s, as shown in Fig. 6(c). As a

result, the spatial phase difference obtained by using the SW-based method, ϕ_{bySW}, can be calculated to be 231° or 129°, which are symmetric about π. However, only one of these is real.

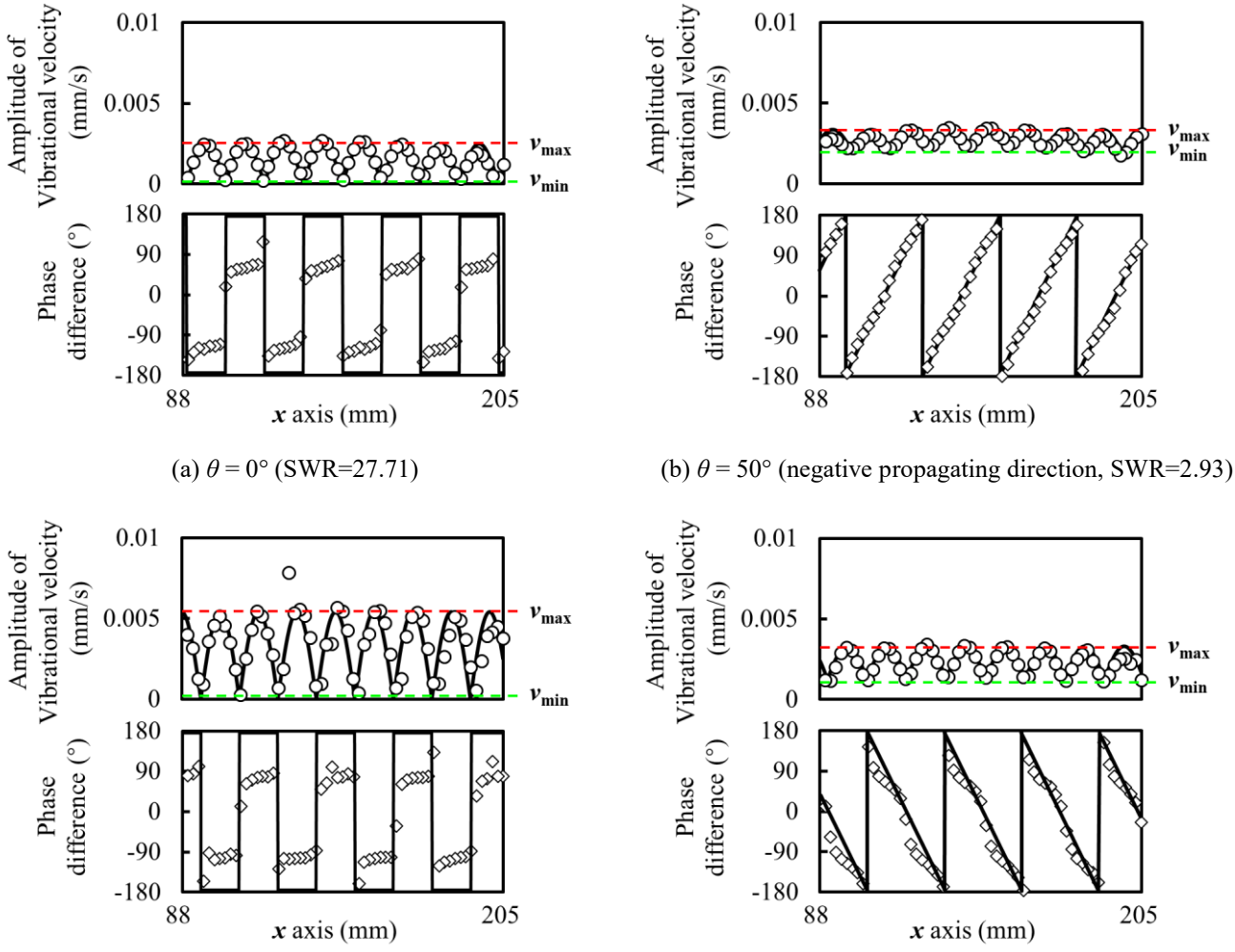

(a) θ = 0° (SWR=27.71)

(b) θ = 50° (negative propagating direction, SWR=2.93)

(c) θ = 180° (SWR= 70.08)

(d) θ = 310° (positive propagating direction, SWR= 4.03)

Fig. 6. Averaged amplitude and phase difference distributions of the vibration velocities along the vibrating plate (in the *x* direction).
(*f*=32.846kHz, *L*=300mm, *V*pp=30V, where θ=0°, 50°, 180°, 310° in graphs (a) to (d) respectively, where the solid lines represent the theoretical values, and the hollow circles and squares represent the experimental values of velocity and phase respectively)

5.2 Measurement of ϕ using the TW-based method

Alternatively, ϕ can also be obtained from (10) using the values of θ, when the TWs were generated. In this way, by changing the temporal phase from 0 to 2π, in intervals of 10 degrees, $\hat{v}_{max}$ and $\hat{v}_{min}$, determined as a function of θ were acquired by using the scanning LDV, and the results were plotted in Fig. 7. Here the blue and the red squares represent the measured values of $\hat{v}_{max}$ and $\hat{v}_{min}$ respectively, while the lines denote the corresponding theoretical values, which were calculated from (8). As can be seen from the figure, these values fit well with the (co-)sinusoidal function shown in the graph. Additionally, $\hat{v}_{max}$ and $\hat{v}_{min}$ can be seen to have reached their closest values at θ_1=50° and θ_2=310°, which are symmetric about π, in accordance with the TW conditions given from (10) and (11). To verify that the TWs are generated, the averaged amplitude and phase difference distributions, both obtained from the LDVs, of the vibration velocities along the vibrating plate are shown in Fig. 6. As can be seen in Fig. 6 (b) (d), where θ equals 50°

and 310°, the phase difference of the vibrational velocity periodically changes from -π to π along the vibrating plate, implying that the component of the TWs reaches its maximum[28]. Thus, with the resulting phase shift θ_1 and its negative propagating direction, the value of ϕ_{byTW} is given by 230°, by using the TW-based method.

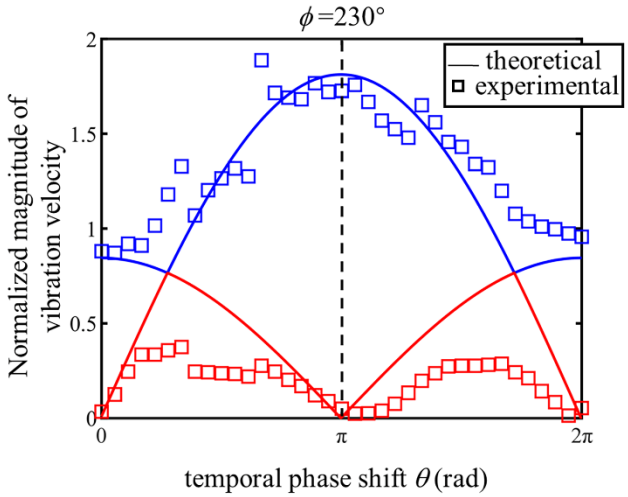

Fig. 7. v_{max}, v_{min} plotted against θ, varying from 0 to 2π. (in increments of 10 degrees (where the blue and red colored squares represent experimental values of v_{max} and v_{min} respectively, and the corresponding blue and red lines denote the theoretical values, where ϕ = 230°)

By comparison to the method developed by the authors and described here, in the traditional method ϕ is usually calculated directly from its definition (and given by ϕ_{byDef}, where $\phi = k(L\text{-}n\lambda)$), and in the case where L = 300mm, this means that the value of ϕ_{byDef} is equal to 257°. The values obtained by using both the traditional method and the method developed here show a deviation one from the other, which indicates that the traditional approach used to join the transducers and the vibrating plate leads to an inaccuracy in these values. Thus, the measurement of the *actual* spatial phase difference, ϕ, is essential for an accurate result for the SWR to be obtained, where this can be further adjusted in this transportation system by using a knowledge of ϕ.

6. Conclusion

In this study, the relationship across θ, ϕ and the SWR has been investigated by the authors for the first time and it is clear that this then can be used for controlling the speed and direction of the transportation system. For such an operating of a dual transducer-type ultrasonic levitation-based transportation system, it is preferential to adjust θ to change the value of the SWR. To do so, ϕ should be obtained in advance. Therefore, two methods to measure ϕ have been proposed: one allows the calculation of ϕ by measuring the amplitude of the pure SWs formed on the vibrating plate; the other method requires finding the value of θ that makes the component of the TWs reach the maximum, therefore allowing the calculation of ϕ from the value of θ. As a result, the amplitude and phase of the vibrational velocity along a vibrating plate of 300mm in length was measured experimentally using the LDVs. By varying θ from 0 to 2π, both the TW condition and the SW condition were obtained, and the two methods of measuring ϕ are verified. Thus, from any of these conditions, an accurate value of ϕ can be calculated, using the relationship across θ, ϕ and the SWR developed and illustrated in this paper by the authors.

Acknowledgments

This work was supported by Self-Planned Task (No. SKLRS202003B) of State Key Laboratory of Robotics and System, Harbin

Institute of Technology. Grattan and Sun acknowledge support from the Royal Academy of Engineering.

References

[1] R. Gabai, R. Shaham, S. Davis, N. Cohen, I. Bucher, A Contactless Stage Based on Near-Field Acoustic Levitation for Object Handling and Positioning-Concept, Design, Modeling, and Experiments, IEEE-ASME Trans. Mechatron. 24 (2019). https://doi.org/10.1109/TMECH.2019.2935428.

[2] K.H. Park, K.Y. Ahn, S.H. Kim, Y.K. Kwak, Wafer distribution system for a clean room using a novel magnetic suspension technique, IEEE-ASME Trans. Mechatron. 3 (1998). https://doi.org/10.1109/3516.662871.

[3] J.K. Park, P.I. Ro, Noncontact manipulation of light objects based on parameter modulations of acoustic pressure nodes, J. Vib. Acoust.-Trans. ASME 135 (2013). https://doi.org/10.1115/1.4023816.

[4] M.A.B. Andrade, N. Pérez, F. Buiochi, J.C. Adamowski, Matrix method for acoustic levitation simulation, Ultrason. Ferroelectr. Freq. Control 58 (2011). https://doi.org/10.1109/TUFFC.2011.1995.

[5] T. Kozuka, T. Tuziuti, H. Mitome, T. Fukuda, Control of a standing wave field using a line-focused transducer for two-dimensional manipulation of particles, Jpn. J. Appl. Phys. 37 (1998). https://doi.org/10.1143/jjap.37.2974.

[6] D. Foresti, M. Nabavi, D. Poulikakos, Contactless transport of matter in the first five resonance modes of a line-focused acoustic manipulator, J. Acoust. Soc. Am. 131 (2012). https://doi.org/10.1121/1.3672700.

[7] D. Koyama, K. Nakamura, Noncontact ultrasonic transportation of small objects in a circular trajectory in air by flexural vibrations of a circular disc, Ultrason. Ferroelectr. Freq. Control 57 (2010). https://doi.org/10.1109/TUFFC.2010.1562.

[8] T. Hoshi, Y. Ochiai, J. Rekimoto, Three-dimensional noncontact manipulation by opposite ultrasonic phased arrays, Jpn. J. Appl. Phys. (2014). https://doi.org/10.7567/JJAP.53.07KE07.

[9] Y. Ochiai, T. Hoshit, J. Rekimoto, Pixie dust: Graphics generated by levitated and animated objects in computational acoustic-potential field, ACM Trans. Graph. (2014). https://doi.org/10.1145/2601097.2601118.

[10] Y. Ochiai, T. Hoshi, J. Rekimoto, Three-dimensional mid-air acoustic manipulation by ultrasonic phased arrays, PLoS ONE. 9 (2014). https://doi.org/10.1371/journal.pone.0097590.

[11] D. Foresti, M. Nabavi, M. Klingauf, A. Ferrari, D. Poulikakos, Acoustophoretic contactless transport and handling of matter in air, Proc. Natl. Acad. Sci. 110 (2013). https://doi.org/10.1073/pnas.1301860110.

[12] D. Foresti, G. Sambatakakis, S. Bottan, D. Poulikakos, Morphing surfaces enable acoustophoretic contactless transport of ultrahigh-density matter in air, Sci. Rep. 3 (2013). https://doi.org/10.1038/srep03176.

[13] R. Kashima, S. Murakami, D. Koyama, K. Nakamura, M. Matsukawa, Design of a junction for a noncontact ultrasonic transportation system, Ultrason. Ferroelectr. Freq. Control. 61 (2014). https://doi.org/10.1109/TUFFC.2014.2998.

[14] K. Nakamura, D. Koyama, Non-contact transportation system of small objects using Ultrasonic Waveguides, in: IOP Conference Series: Materials Science and Engineering, 2012. https://doi.org/10.1088/1757-899X/42/1/012014.

[15] Y. Ito, D. Koyama, K. Nakamuray, High-speed noncontact ultrasonic transport of small objects using acoustic traveling wave field, Acoust. Sci. Techno. 31 (2010). https://doi.org/10.1250/ast.31.420.

[16] M. Ding, D. Koyama, K. Nakamura, Noncontact ultrasonic transport of liquid using a flexural vibration plate, Appl. Phys. Express 5 (2012). https://doi.org/10.1143/APEX.5.097301.

[17] Y. Hashimoto, Y. Koike, S. Ueha, Transporting objects without contact using flexural traveling waves, J. Acoust. Soc. Am. 103 (1998). https://doi.org/10.1121/1.423039.

[18] P. Smithmaitrie, P. Suybangdum, P. Laoratanakul, N. Muensit, Design and performance testing of an ultrasonic linear motor with dual piezoelectric actuators, Ultrason. Ferroelectr. Freq. Control. 59 (2012). https://doi.org/10.1109/TUFFC.2012.2289.

[19] B. Dehez, C. Vloebergh, F. Labrique, Study and optimization of traveling wave generation in finite-length beams, Math. Comput. Simul. 2010. https://doi.org/10.1016/j.matcom.2010.05.013.

[20] G.H. Kim, J.W. Park, S.H. Jeong, Analysis of dynamic characteristics for vibration of flexural beam in ultrasonic transport system, J. Mater. Sci. Technol. 23 (2009). https://doi.org/10.1007/s12206-008-1219-6.

[21] B.G. Loh, P.I. Ro, An object transport system using flexural ultrasonic progressive waves generated by two-mode excitation, Ultrason. Ferroelectr. Freq. Control. 47 (2000). https://doi.org/10.1109/58.852083.

[22] T. Ide, J. Friend, K. Nakamura, S. Ueha, A non-contact linear bearing and actuator via ultrasonic levitation, Sens. Actuator A-Phys. 135 (2007). https://doi.org/10.1016/j.sna.2006.08.005.

[23] T. Ide, J.R. Friend, K. Nakamura, S. Ueha, A Low-Profile Design for the Noncontact Ultrasonically Levitated Stage, Jpn. J. Appl. Phys. 44 (2005). https://doi.org/10.1143/jjap.44.4662.

[24] D. Koyama, T. Ide, J.R. Friend, K. Nakamura, S. Ueha, An ultrasonically levitated noncontact stage using traveling vibrations on precision ceramic guide rails, Ultrason. Ferroelectr. Freq. Control. 54 (2007). https://doi.org/10.1109/TUFFC.2007.282.

[25] K. F. Graff, Wave motion in elastic solid, Dover, New York, 1991.

[26] H.J. Dong, J. Wu, G.Y. Zhang, H.F. Wu, An improved phase-locked loop method for automatic resonance frequency tracing based on static capacitance broadband compensation for a high-power ultrasonic transducer, Ultrason. Ferroelectr. Freq. Control. 59 (2012). https://doi.org/10.1109/TUFFC.2012.2180.

[27] J. Wu, Y. Mizuno, K. Nakamura, Polymer-Based Ultrasonic Motors Utilizing High-Order Vibration Modes, IEEE-ASME Trans. Mechatron. 23 (2018). https://doi.org/10.1109/TMECH.2018.2794379.

[28] K. Masuda, D. Koyama, M. Matsukawa, Noncontact Transportation of Planar Object in an Ultrasound Waveguide, IEEE Trans. Ultrason. Ferroelectr. Freq. Control. (2018). https://doi.org/10.1109/TUFFC.2018.2870069.